Hydrogen radiolytic release from zeolite 4A/water systems under γ irradiations

Laëtitia Frances, Manuel Grivet, Jean-Philippe Renault, Jean-Emmanuel Groetz, Didier Ducret

Title:

Hydrogen Radiolytic Release from Zeolite 4A / Water Systems Under γ Irradiations

Authors:

FRANCES Laëtitia *[a,c], GRIVET Manuel [a], RENAULT Jean-Philippe [b], GROETZ Jean-Emmanuel [a], DUCRET Didier [c]

**corresponding author:* lfrances@univ-fcomte.fr

Affiliations:

[a] MCF. M. Grivet (mgrivet@univ-fcomte.fr), MCF J.E. Groetz (jean-emmanuel.groetz@univ-fcomte.fr), L. Frances*
Université de Franche-Comté, Laboratoire Chrono-Environnement (UMR CNRS 6249),
25030 Besançon Cedex (France)
Fax: (+33) 3-8166-6522

[b] Dr. J.P. Renault (jean-philippe.renault@cea.fr)
CEA/Saclay, DSM/DRECAM/SCM/URA 331 CNRS
91191 Gif-Sur-Yvette Cedex (France)

[c] Dr. D. Ducret (didier.ducret@cea.fr) , L. Frances*
CEA/Valduc, Département TRItium
21120 Is-sur-Tille (France)

Abstract:

Although the radiolysis of bulk water is well known, some questions remain in the case of adsorbed or confined water, especially in the case of zeolites 4A, which are used to store tritiated water. An enhancement of the production of hydrogen is described in the literature for higher porous structures, but the phenomenon stays unexplained. We have studied the radiolysis of zeolites 4A containing different quantities of water under ^{137}Cs gamma radiation. We focused on the influence of the water loading ratio. The enhancement of hydrogen production compared with bulk water radiolysis has

Abbreviations :

WLR : Water Loading Ratio
ZWS : Zeolite 4A / Water System

been attributed to the energy transfer from the zeolite to the water, and to the influence of the water structure organization in the zeolite. Both were observed separately, with a maximum efficiency for energy transfer at a loading ratio of about 13%, and a maximum impact of structuration of water at a loading ratio of about 4%.

Keywords:

⇒ Zeolite
⇒ Adsorbed water
⇒ Radiolysis
⇒ Hydrogen
⇒ Molecular sieve
⇒ Microporous

1. Introduction:

Zeolites are widely used nanoporous materials. They are encountered in a broad field of applications, such as catalysis, filtration and isotopic separation (Kotoh et al., 2010, 2009; Montanari and Busca, 2008; Zhu et al., 2005). Zeolites A, which are hydrophilic, are also used to store tritiated water, generated and required by nuclear applications like ITER. This experimental reactor is supposed to produce, amongst other tritiated wastes, high quantities of pure tritiated water during its working period (Pamela et al., 2013). Its development requires safe storage solutions.

Synthetic Zeolites A are built with corner sharing TO_4 tetrahedrons, where T corresponds to silicon or aluminum (Breck, 1974). At the nanometer scale, their crystalline structure is composed of two kinds of cages. Sodalite cages, also called β cages, are a truncated octahedral shape, with a diameter of 6.6 Å, disposed at each corner of a cubic arrangement. The second kind of cages, called supercages or α cages, are located in the center of this array, and are characterized by a diameter of 11.4 Å. Sodalites cages are linked together by prisms, called double-four-membered rings (D4R). The framework negative charge (induced by the aluminum valence) is compensated by cations, included in the structure. The nature and location of those cations affects the properties of the zeolite. In zeolites 4A, the positive charge is provided by monovalent sodium cations, leading to the following chemical composition for a unit cell: $[Na_{12}(SiO_4)_{12}(AlO_4)_{12}]$. The zeolite 4A is strongly hydrophilic. A unit cell can adsorb 27 molecules of water. Among those 27 molecules, some are commonly localized as molecules adsorbed in the crystalline structure: 4 or 5 in each sodalite cage and 20 to 23 in each supercage (Crupi et al., 2005; Demontis et al., 2008).

The quantity of water is expressed as Water Loading Ratio (WLR) given in percentage, equal to the mass of water divided by the mass of zeolites. The maximum loading ratio for zeolites 4A depends on the synthesis method and the binder quantity, but is about 20 %. It has been shown, considering the adsorption heat (Moïse et al., 2001) or FTIR results (Crupi et al., 2003), that the water adsorption is heterogeneous, and occurs in three-steps, leading to different kinds of confined water. The first adsorbed water molecules solvate the cations which then migrate, opening the access to the β cages. The α cages are then filled.

Even if bulk water radiolysis is well known, even in the case of self-radiolysis of tritiated water (Buxton et al., 1988; Ershov and Gordeev, 2008), (Stolz et al., 2003), many questions remain about the radiolysis of adsorbed and confined water. An enhancement of hydrogen production, in some porous materials has been observed, for different irradiation conditions (Cecal et al., 2004; Le Caër, 2011; Le Caër et al., 2005; Rotureau et al., 2005). The same phenomenon is observed in the precise case of zeolites A (Nakashima and Aratono, 1993; Nakashima and Tachikawa, 1987), or structurally-closed zeolites: faujasites (Nakashima and Masaki, 1996), but the literature is quite limited in this area, even if the impact of confinement on radiolysis has been shown (Foley et al., 2005).

Since the interaction and behavior of water strongly depends on the loading ratio of zeolites, we followed gas production depending on the level of water filling of the zeolites. We chose gamma irradiations, which are close to β^- irradiations induced by tritiated water in terms of the dose rate. We took special care with respect to the dosimetry: the primary energy deposition in water is commonly estimated to be equal to the total energy deposited multiplied by its mass ratio (LaVerne and Tandon, 2002),(LaVerne and Tonnies, 2003). We proposed an improvement of this consideration using Monte-Carlo simulation. We focused on the dihydrogen production since it may create, with dioxygen, an explosive atmosphere over a large range of concentration. We adopted two different approaches, regarding both primary energy deposition in the water and energy deposition in the whole system containing zeolites 4A and water.

2. Materials and Methods

2.1.Sample conditioning

Synthetic hydrophilic zeolites 4A were supplied by Molsiv Adsorbents. Their maximum water capacity, expressed as the ratio of water mass under dried zeolite mass, given by the supplier is 19.6 %. To improve the mechanical properties of zeolites 4A, a chemical inert non-porous binder, presenting the same atomic composition as the zeolites, is included during the synthesis. We estimated the proportion of binder by comparing the experimental water quantity adsorbed at

saturation for our samples and that for a pure 4A sample, provided by CECA. The water saturation obtained by exposure to ambient water vapor, is investigated by thermogravimetry and is obtained as a mass percentage of 25 % for pure zeolites, against 19 % for our storage samples. The binder proportion is so estimated to be 24 %. Nevertheless, as the atomic composition of binder is close to the one of pure zeolites, no significant influence on interaction sections, and thus on irradiation effects, is expected.

4 g of zeolites 4A were introduced in 10 cm^3 air tight glass ampoules. Samples were then conditioned with a unique bench, comprising a pump, a pure water tank, a manometer and a junction to connect ampoules containing samples (figure 1). The use of a unique bench and of a unique ampoule for the different steps of samples conditioning prevents from the exposition of zeolites 4A to atmospheric water. As they are hydrophilic, such an exposition would have led to residual water adsorption by zeolites.

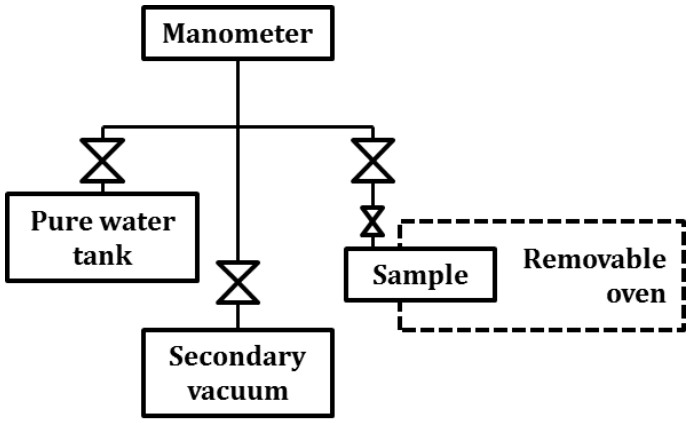

Figure 1. Schematic representation of the bench used to adsorb controlled amounts of water.

Each ampoule was degassed under vacuum at 623 K, during at least 12 h, to ensure the elimination of water from zeolites initially equilibrated with water vapor from the atmosphere. The complete dehydration has been checked by weighing, after isolation and removal of ampoules from the bench. Adsorption of controlled quantity of water, from about 3 % to saturation, was realized by manometry. Zeolites were exposed to the chosen water vapor pressure, released in the line whose volume has been measured to 2.58 dm^3. The quantity of water adsorbed was thus pre-determined using the perfect gas equation, and checked by the mass increase. Details of the quantities of water adsorbed are given in Table 1.

Water loading ratio (%)	3.1	4.1	5.6	7.1	13.0	19.1
F [a]	1.50	1.53	1.52	1.50	1.46	1.43
E_{water} (%)[b] (from mass ratio)	3.0	3.9	5.3	6.6	11.5	16.0
E_{water} (%)[b] (improved with MCNPX)	4.9	6.1	8.1	10.3	17.4	23.6

[a] *Correction coefficient used to calculate total energy deposited in zeolite/water systems from energy deposited in the Fricke dosimeter*

[b] *Percentage of total energy deposited in water*

Table 1. Characteristics of irradiated zeolite 4A / water systems

Ampoules were then connected to the analysis bench, and filled with argon, used as gas carrier during irradiations and analysis, with a pressure of 1.46 bar. Each sample underwent several irradiations. The analysis line is also used to replace radiolysis gases after each irradiation and each measure, by pure argon. We then proceeded with the following irradiation.

2.2. Irradiations

γ irradiations by a ^{137}Cs source were carried out with a dose rate of 5.4 $Gy.min^{-1}$. The experimental dose was determined by irradiation using the Fricke dosimeter, irradiated under the same conditions as the zeolites samples (equivalent mass, equivalent ampoule and equivalent volume).

After the initial conditioning, consisting in water adsorption at controlled ratios, each ampoule underwent several cycles of irradiations. One cycle includes a filling with argon, used as the carrier gas, exposition to the ^{137}Cs source, analysis of the gas released, elimination of radiolysis gases, and weighing. This last step is carried out successfully to ensure that the quick elimination of radiolysis gases under primary vacuum did not induce significant modifications of the amount of water adsorbed. Samples have been exposed to radiations during periods from 14 hours to 63 hours. The apparent quantity of hydrogen produced was determined by gas chromatography (Varian model CP 2003), using argon as the carrier gas. Chromatogram peaks were integrated with the software Soprane. Calibration of the chromatograph was performed using a dedicated standard gas, containing argon, and H_2, in a known concentration of 99.6 ppm. The error on the H_2 concentration measure, in ppm, was calculated to be 2 %.

The absence of any significant hydrogen release under irradiation has been checked for empty glass ampoules and for an ampoule containing dried zeolites 4A.

3. Results and discussion:

Six systems containing the same quantity of zeolites (about 3.5 g) but with different quantities of water underwent cumulative γ irradiations. The quantity of hydrogen released was measured after each irradiation, and eliminated before the next one.

3.1. Dosimetry

The energy deposition is commonly deduced from the Fricke dosimetry (LaVerne and Tandon, 2002; LaVerne and Tonnies, 2003; Le Caër et al., 2005). However, if the Fricke dosimeter is relevant for homogenous systems, its precision for heterogeneous systems is debatable. Discussion about energy transfers also requires a precise idea of how primary energy deposition is divided between the zeolites and water. This repartition is frequently evaluated from the weight ratio (LaVerne and Tandon, 2002; LaVerne and Tonnies, 2003), which does not take into account the different composition between the adsorbent and the adsorbed molecules. The different atomic composition between zeolites and water implies, for example, different interaction cross sections, physical and electronic densities. Therefore, we conducted Monte-Carlo simulations, to improve the evaluation of the dose deposition in the systems, in zeolites and in water, rather than considering untreated experimental dosimetry results and mass ratios.

The experimental dose deposed in the samples, is experimentally estimated from the dose deposited in the Fricke dosimeter, exposed to gamma radiation, in similar conditions (equivalent mass, equivalent geometry, and equivalent volume) to the Zeolite / Water Systems (ZWS). The experimental dose rate is thus estimated to be 5.4 $Gy.min^{-1}$.

To calculate the energy deposited in the samples, as a function of water loading, we carried out simulations with the MCNPX code, version 2.7.0, based on Monte-Carlo considerations. MCNPX is able to follow gamma particles and secondary electrons generated. It evaluates the statistical energy deposition and location until a threshold of 1 keV. Under this energy, the program consider that the energy carried by the particles is deposited where it is locate. A model of two spheres was used (figure 2). The first sphere contains the water and the second sphere has the interaction properties of zeolites, that is to say, the atomic composition and density (1.57) of zeolites 4A. For each system, the diameter of the water sphere has been calculated to provide a volume ratio between the zeolite and water corresponding to their mass ratio, considering their respective density. If r_w, on figure 2,

represents the radius of the water sphere and is directly linked to the water mass and volume, R represents the radius of the bigger sphere, but is not directly linked to zeolite mass and volume, as water replaces zeolite material in the geometry. The ratio between r_w and R have been calculated for the different quantities of water adsorbed.

We indicated a density of 1 for water and 1.57 for zeolites and atomic composition of zeolites and water is given as an input parameter. Results are given for 10^8 gamma followed.

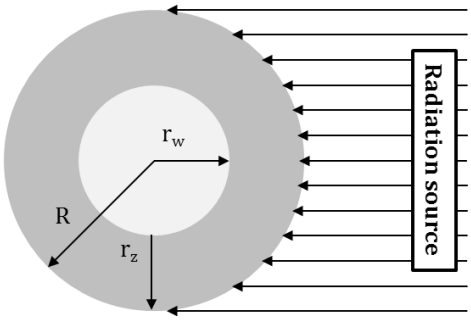

$$\frac{R}{r_w} = \sqrt[3]{\frac{1}{WLR} \times \frac{\rho_{eau}}{\rho_{Z4A}} + 1}$$

Figure 2. Geometry used with MCNPX with radius details, to estimate energy depositions in water and in zeolites, from Fricke dosimeter.

Using the Fricke dosimeter, MCNPX gave a correction coefficient called F (table 1) for energy deposition in the whole sample, slightly evolving with the water loading. Simulation also provides, for each one of the six systems studied, an indication about the energy distribution between the zeolite and the water. This distribution concerns first the energy deposition events and does not take into account the energy transfer occurring after them. The primary energy deposition in water (E_{water}) is given as a percentage in table 1. It does not imply a drastic change compared to primary energy deposition calculated from mass ratios. Note that the energy deposition in percentage calculated from the water mass ratio is different from the Water Loading Ratio. Actually, the latter is conventionally defined as the mass of water divided by the mass of dried zeolites. Energy deposition has to be calculated from the ratio between the mass of water and the total mass of the system.

3.2. Hydrogen production

Using these simulation results, we extracted two kinds of information from the hydrogen release, one according to the energy deposition in the whole system, and a second according to the primary

energy deposited in the water. The first one consists in considering the extreme case of a complete energy transfer from the zeolite to the adsorbed water. The second one consists in neglecting this energy transfer. Following this second strategy, we obtained a hydrogen release which can be compared to hydrogen measured in free bulk water. This quantity of hydrogen is calculated from the primary radiolytic yield encountered in the literature: 0.045 µmol.J^{-1} (Rotureau et al., 2005). Our measurements first confirmed the enhancement of hydrogen production that can be multiplied by three in the presence of the zeolites, previously described as a catalyst (Cecal et al., 2004).

As observed by Nakashima et al. (Nakashima and Aratono, 1993; Nakashima and Tachikawa, 1987), hydrogen release seems to be linearly dependent on the energy deposited for the higher water loading ratios (higher than 12~13 %) (figure 3). This behavior is conserved for lower loading (figure 4), contrary to the results available for 5A zeolites (Nakashima and Tachikawa, 1987) that showed a slow-down of the hydrogen release rate with respect to the dose deposition. In the case of 5A zeolites, irradiations were carried out in one-step, with different irradiations stages. In our case we exposed ZWS repeatedly to irradiations, eliminating hydrogen between the two steps.

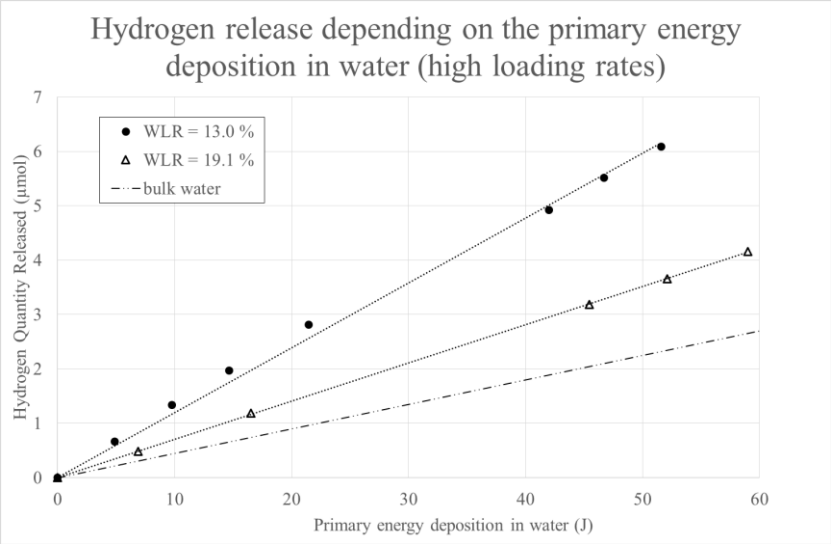

Figure 3. Cumulated hydrogen released from ZWS, depending on the cumulated primary energy deposition in water, for water loading ratios between 10 and 20%. The dashed line shows the quantity of hydrogen which would have been released for free water irradiated under similar conditions. (WLR: Water Loading Ratio)

Figures 3 and 4 represent the total hydrogen released depending on the total energy deposited in the water. The elimination of the hydrogen ensures that the system returns to its initial state between each irradiation. This in turn avoids hydrogen recombination that is observed at high doses, when a single long irradiation is carried out rather than cumulated ones. The lower hydrogen quantity observed for our longest segmented irradiations, corresponds to the slowing down observed by Nakashima et al. along one-step irradiations.

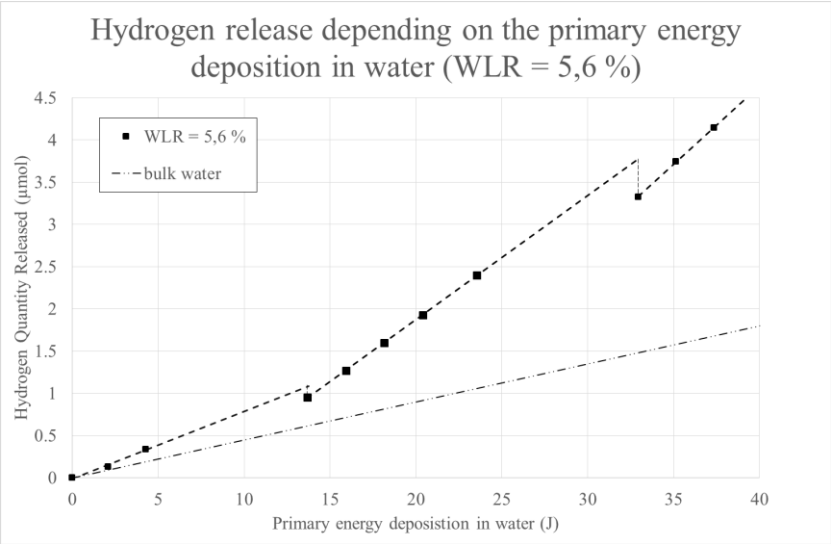

Figure 4. Hydrogen released from ZWS, depending on the primary energy deposition in water, for the water loading ratio of 5.6%. The dashed line shows the quantity of hydrogen which would have been released for free water irradiated under similar conditions. (WLR: Water Loading Ratio)

Otherwise, after our long-step irradiations, for the lower loading ratios, a slight increase is observed for the hydrogen release ratio (figure 4). Similar results are obtained if the energy deposition in the whole ZWS is taken into account.

3.3. Hydrogen radiolysis yield

For each water loading ratio, the hydrogen radiolytic yields are extracted from the slopes between two consecutive points. Values obtained for similar slopes are joined to calculate the average hydrogen radiolytic yield. When they are not compatible, two radiolytic yields are calculated and extracted.

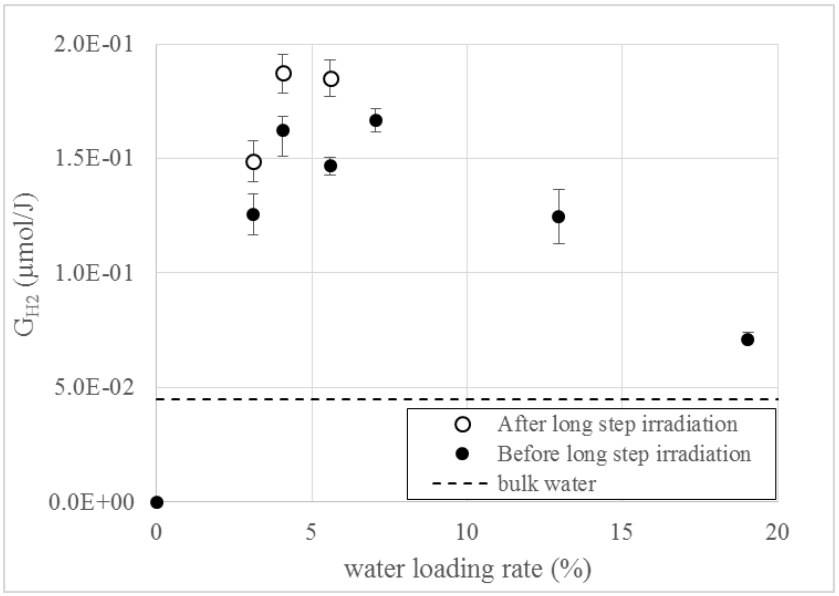

Figure 5. Apparent hydrogen radiolytic yield as a function of the water loading ratio of zeolites, according to the primary energy deposition in water.

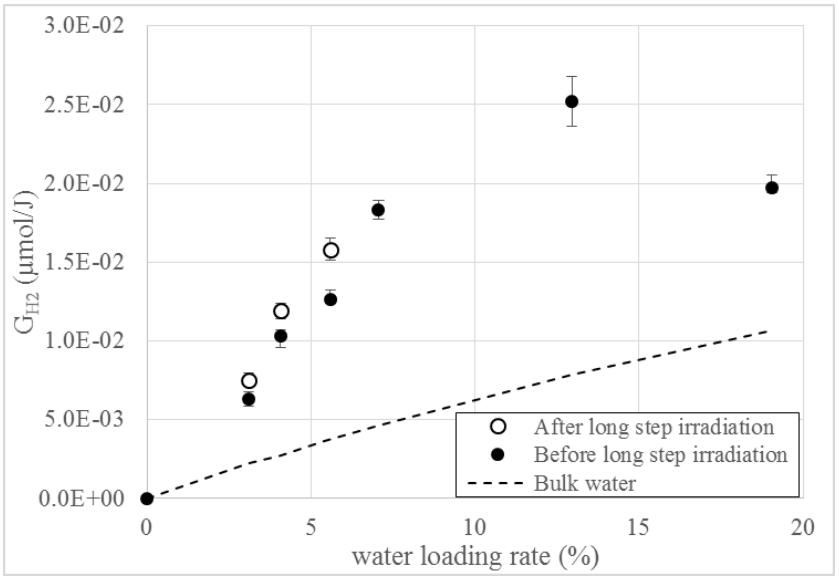

Figure 6. Apparent hydrogen radiolytic yield as a function of the water loading ratio of zeolites, according to the energy absorbed by the whole system (zeolites 4A and water)

The calculated hydrogen radiolytic yields, using the two strategies previously described are given in figure 5 and 6. The dashed line in figure 5 shows the reference value for irradiated bulk water irradiated under similar conditions (primary hydrogen radiolytic yield: 0.045 $\mu mol.J^{-1}$). The dashed line in figure 6 represents the apparent G value calculated from the bulk water radiolytic yield, for the irradiation of a ZWS system, with the total energy deposition taken into account, but without energy transfer from the zeolite.

In both cases, whatever the energy taken into account, hydrogen release seems to be favored in ZWS systems compared to free bulk water. Nevertheless, the yield does not increase linearly with the WLR. A maximum appears and its position depends on whether the radiolytic yield is calculated from the primary energy deposition in the water or in the whole system.

The hydrogen radiolytic yield, calculated from the primary energy deposition in water, shows a maximum for a loading ratio close to 4 %, and then decreases, approaching the yield obtained in water (figure 5). This loading ratio corresponds to a particular hydration condition of the zeolite. At a loading ratio of 4 %, β cages are filled and the water adsorbed is the water which presents the strongest interaction with the zeolite. This is highlighted by the conditions required to evacuate this water. Dehydration of the zeolite from saturation to 4 or 5 % is possible by pumping under secondary vacuum for several hours. Then, to eliminate the residual water, additional heating over 423 K is required (Demontis et al., 2008). Besides, the entropy of the water adsorbed in β^- cages is close to the entropy of solid water at absolute zero temperature (Mizota et al., 2001). This illustrates the confinement effect on the organization of water. The strong confinement effect and interaction between zeolite and water at such a loading rate seems to favor energy transfer and dihydrogen production.

The hydrogen radiolytic yields calculated from the energy deposited in the whole ZWS shows a different maximum, at a WLR of 13 % (figure 6). If the transfer of energy from zeolite to water is complete, the hydrogen radiolytic yield should vary in the same way than the radiolytic yield calculated for the primary energy deposition in water. The maximum obtained at 13% highlights a maximum efficiency of all cumulated interactions between zeolite and water. It is coherent with the hydration of the zeolite. Actually, above 13 %, water adsorbed in zeolites, is sometimes called “bulk-like” water, as it is located in the center of α cages, and only undergoes a low indirect influence from the zeolite (Demontis et al., 2008). At about 13 %, the maximum internal surface coverage is reached, leading to a configuration in which the higher proportion of water interacts with the zeolite. It seems that the more the internal surface of the zeolite is covered by water, the more efficient the

energy transfer is. Then, for higher WLR, the hydrogen radiolytic yield decreases tending to join that for bulk water.

If the confinement effects are neglected, we can evaluate the percentage of energy transferred from the zeolite to water at the end of the irradiation stages, by assuming that the hydrogen radiolytic yield of adsorbed water would be equal to the one in bulk water (0.045 µmol.J^{-1}).

Results are given in table 2. "p" is the percentage of energy transferred from the zeolite to water, compared to the quantity of energy deposited in the zeolite. "n_{H2}" is the quantity of hydrogen released, "G_{H2}" the radiolytic yield of dihydrogen in water, "E_{water}" the primary energy deposition in water and "$E_{zeolite}$" the primary energy deposition in zeolite.

WLR (%)	3.1	4.1	5.6	7.1	13.0	19.1
E_{system} (J)	388.3	455.5	461.3	208.5	296.5	250.1
$E_{zeolite}$ (J)	369.3	427.7	423.9	187.0	244.9	191.1
E_{water} (J)	19.0	27.8	37.4	21.5	51.6	59.0
$n_{H2\ total}$ (µmol)	1.57	3.14	4.14	2.45	6.09	4.16
p (%)	4.3	9.8	12.9	17.6	34.2	17.5
G_{H2} (µmol.J^{-1})[a]	6.2×10^{-3}	9.9×10^{-3}	1.2×10^{-2}	1.7×10^{-2}	2.2×10^{-2}	1.7×10^{-2}

[a] : calculated according to the energy deposition in the whole system and excluding the long step irradiations which slow down the hydrogen production

Table 2. Evaluation of the energy transfer from the zeolite to the water according to water loading ratios in our systems.

The maximum percentage of energy transferred, evaluated this way, is about 34 %, for the WLR of 13.0 %. This value is high compared to the energy transferred from CeO_2 or ZrO_2 to adsorbed water, which are of 4 and 18 % respectively, and which are calculated with the same reasoning (LaVerne and Tandon, 2002). This comparison tends to confirm that energy transfers from zeolite to adsorbed water are efficient.

Moreover, the confinement effect has been shown to favor the radiolysis in controlled pore glasses (Foley et al., 2005). Our result, obtained for smaller cavities, is consistent with these observations, as G_{H2} calculated from the energy deposition in water shows a maximum for a complete filling of the smallest cavity, where the water is in the most organized state. For this loading ratio, according to the

strength of interaction between zeolite and adsorbed water, confinement could result in a quasi-immobilization of water. This interpretation is confirmed by a decrease tending to the value of the hydrogen radiolytic yield obtained for bulk water, when the loading ratio increases, and so the strength of the interaction between zeolite and water, and the confinement effects decrease.

Nevertheless, the specific state of confined/fixed water does not simply correspond to a high organization of water, if we compare the radiolysis of liquid water and radiolysis of ice water. Actually, the radiolytic yield of hydrogen in ice under gamma radiation is much lower than in liquid water, with values such as 0.007 $\mu mol.J^{-1}$ at -196°C, 0.010 $\mu mol.J^{-1}$ at -100°C and 0.026 $\mu mol.J^{-1}$ at -15°C (Ghormley and Stewart, 1956; Siegel and Rennick, 1966). Freezing and increasing the organization of water seems to decrease the hydrogen radiolytic yield rather than favoring it. A modification of the migration properties of the intermediate species of radiolysis in confined water could also be implied. It would lead to a perturbation of the recombination mechanisms, resulting in the excessive production of hydrogen compared to free liquid water.

4. Conclusion:

Hydrogen released has been quantified for different Zeolites 4A/ Water Systems (ZWS), containing different water quantities. An enhancement of hydrogen production in ZWS compared to bulk water has been first confirmed. The influence of the water loading ratio (WLR) on the hydrogen released by radiolysis has been studied with two approaches.

A maximum hydrogen radiolytic yield is observed at a WLR of about 4 %, if the primary energy deposition in water is used for the calculations. In this configuration, water is confined in the β cages, in the most organized configuration, and undergoes the strongest interaction with the zeolites. It seems that the strongest interaction leads to the highest hydrogen radiolytic yield. β cages water shows the most efficient hydrogen production under radiolysis by gamma radiation.

If the energy deposition in the whole system is used, the maximum hydrogen radiolytic yield is displaced to 13 % WLR. This results reveals the WLR that shows the most efficient hydrogen production, when cumulated interactions are taken into account. The 13 % WLR value, corresponding to a maximum coverage of the inner surfaces of zeolite, is consistent with the hydration of zeolites 4A.

The WLR of 13 % also corresponds to the situation when the gas phase contains the most important concentration of hydrogen, in absolute value, during the radiolysis under gamma radiations.

5. Acknoledgment:

We acknowledge the CEA (Commissariat à l'Energie Atomique et aux Energies Alternatives) for financial support. We also acknowledge the LICB (Laboratoire Interdisciplinaire Carnot de Bourgogne) for their help in understanding the behavior of zeolites.

6. References

Breck, D.W., 1974. Zeolite molecular sieves: structure, chemistry, and use. R.E. Krieger.

Buxton, G.V., Greenstock, C.L., Helman, P.W., Ross, A.B., 1988. Critical Review of Rate Constants for Reactions of Hydrated Electrons Hydrogen Atoms and Hydroxyl Radicals (OH/O^-) in Aqueous Solution. J. Phys. Chem. 17, 513–885. doi:10.1063/1.555805

Cecal, A., Colisnic, D., Popa, K., Paraschivescu, A.O., Bilba, N., Cozma, D.G., 2004. Hydrogen yield from water radiolysis in the presence of zeolites. Cent. Eur. J. Chem. 2, 247–253. doi:10.2478/BF02476194

Crupi, V., Longo, F., Majolino, D., Venuti, V., 2005. T dependence of vibrational dynamics of water in ion-exchanged zeolites A: A detailed Fourier transform infrared attenuated total reflection study. J. Chem. Phys. 123, 154702. doi:10.1063/1.2060687

Crupi, V., Majolino, D., Migliardo, P., Venuti, V., Wanderlingh, U., 2003. A FT-IR absorption analysis of vibrational properties of water encaged in NaA zeolites: evidence of a structure maker role of zeolitic surface. Eur. Phys. J. E - Soft Matter 12, 55–58. doi:10.1140/epjed/e2003-01-014-4

Demontis, P., Gulín-González, J., Jobic, H., Masia, M., Sale, R., Suffritti, G.B., 2008. Dynamical Properties of Confined Water Nanoclusters: Simulation Study of Hydrated Zeolite NaA: Structural and Vibrational Properties. ACS Nano 2, 1603–1614. doi:10.1021/nn800303r

Ershov, B.G., Gordeev, A.V., 2008. A model for radiolysis of water and aqueous solutions of H_2, H_2O_2 and O_2. Radiat. Phys. Chem. 77, 928–935. doi:10.1016/j.radphyschem.2007.12.005

Foley, S., Rotureau, P., Pin, S., Baldacchino, G., Renault, J.-P., Mialocq, J.-C., 2005. Radiolysis of Confined Water: Production and Reactivity of Hydroxyl Radicals. Angew. Chem. Int. Ed. 44, 110–112. doi:10.1002/anie.200460284

Ghormley, J.A., Stewart, A.C., 1956. Effects of γ-Radiation on Ice. J. Am. Chem. Soc. 78, 2934–2939. doi:10.1021/ja01594a004

Kotoh, K., Takashima, S., Nakamura, Y., 2009. Molecular-sieving effect of zeolite 3A in adsorption of H_2, HD, D_2. Fusion Eng. Des. 84, 1108–1112. doi:10.1016/j.fusengdes.2009.01.052

Kotoh, K., Takashima, S., Sakamoto, T., Tsuge, T., 2010. Multi-component behaviors of hydrogen isotopes adsorbed on synthetic zeolites 4A and 5A at 77.4K and 87.3K. Fusion Eng. Des. 85, 1928–1934. doi:10.1016/j.fusengdes.2010.06.029

LaVerne, J.A., Tandon, L., 2002. H_2 Production in the Radiolysis of Water on CeO_2 and ZrO_2. J. Phys. Chem. B 106, 380–386. doi:10.1021/jp013098s

LaVerne, J.A., Tonnies, S.E., 2003. H_2 production in the Radiolysis of Aqueous SiO_2 Suspensions and Slurries. J Phys Chem B 107, 7277–7280. doi:10.1021/jp0278418

Le Caër, S., 2011. Water Radiolysis: Influence of Oxide Surfaces on H_2 Production under Ionizing Radiation. Water 235–253. doi:10.3390/w3010235

Le Caër, S., Rotureau, P., Brunet, F., Charpentier, T., Blain, G., Renault, J.-P., Mialocq, J.-C., 2005. Radiolysis of Confined Water: Hydrogen Production at a High Dose Rate. ChemPhysChem 6, 2585–2596. doi:10.1002/cphc.200500185

Mizota, T., Petrova, N.L., Nakayama, N., 2001. Entropy of zeolitic water. J. Therm. Anal. Calorim. 64, 211–217. doi:10.1023/A:1011549432295

Moïse, J.C., Bellat, J.P., Méthivier, A., 2001. Adsorption of water on X and Y zeolites exchanged with barium. Microporous Mesoporous Mater. 43, 91–101. doi:10.1016/S1387-1811(00)00352-8

Montanari, T., Busca, G., 2008. On the mechanism of adsorption and separation of CO_2 on LTA zeolites: An IR investigation. Vib. Spectrosc. 46, 45–51. doi:10.1016/j.vibspec.2007.09.001

Nakashima, M., Aratono, Y., 1993. Radiolytic hydrogen gas formation from water adsorbed on type A zeolites. Radiat. Phys. Chem. 41, 461–465. doi:10.1016/0969-806X(93)90005-F

Nakashima, M., Masaki, N.M., 1996. Radiolytic hydrogen gas formation from water adsorbed on type Y zeolites. Radiat. Phys. Chem. 47, 241–245. doi:10.1016/0969-806X(94)00176-K

Nakashima, M., Tachikawa, E., 1987. Radiolytic Gas Production from Tritiated Water Adsorbed on Molecular Sieve 5A. J. Nucl. Sci. Technol. 24, 41–46. doi:10.1080/18811248.1987.9735772

Pamela, J., Bottereau, J.-M., Canas, D., Decanis, C., Liger, K., Gaune, F., 2013. ITER tritiated waste management by the Host state and first lessons learned for fusion development. Fusion Eng. Des. doi:10.1016/j.fusengdes.2013.12.006

Rotureau, P., Renault, J.-P., Lebeau, B., Patarin, J., Mialocq, J.-C., 2005. Radiolysis of Confined Water: Molecular Hydrogen Formation. ChemPhysChem 6, 1316–1323. doi:10.1002/cphc.200500042

Siegel, S., Rennick, R., 1966. Isotope Effects in the 77°K γ Irradiation of Ice. J. Chem. Phys. 45, 3712–3720. doi:10.1063/1.1727391

Stolz, T., Ducret, D., Heinze, S., Baldacchino, G., Colson, J.-C., Dedieu, B., Pelletier, T., 2003. Self radiolysis of tritiated water. Fusion Eng. Des. 69, 57–60. doi:10.1016/S0920-3796(03)00236-9

Zhu, W., Gora, L., Van den Berg, A.W.C., Kapteijn, F., Jansen, J.C., Moulijn, J.A., 2005. Water vapour separation from permanent gases by a zeolite-4A membrane. J. Membr. Sci. 57–66. doi:10.1016/j.memsci.2004.12.039

7. List of figures (all single-column fitting figures)

Figure 1. Schematic representation of the bench used to adsorb controlled amounts of water.

Figure 2. Geometry used with MCNPX with radius details, to estimate energy depositions in water and in zeolites, from Fricke dosimeter.

Figure 3. Cumulated hydrogen released from ZWS, depending on the cumulated primary energy deposition in water, for water loading ratios between 10 and 20%. The dashed line shows the quantity of hydrogen which would have been released for free water irradiated under similar conditions. (WLR: Water Loading Ratio)

Figure 4. Hydrogen released from ZWS, depending on the primary energy deposition in water, for the water loading ratio of 5.6%. The dashed line shows the quantity of hydrogen which would have been released for free water irradiated under similar conditions. (WLR: Water Loading Ratio)

Figure 5. Apparent hydrogen radiolytic yield as a function of the water loading ratio of zeolites, according to the primary energy deposition in water.

8. List of tables